JOURNAL OF MATERIALS SCIENCE 28 (1993) 4497–4502

Study of ferroelectricity in the PMN–PT system near the morphotropic phase boundary

J. C. HO, K. S. LIU, I. N. LIN*
*Department of Materials Science and Engineering, and *Materials Science Centre, National Tsing Hua University, Hsinchu, Taiwan*

The ferroelectric properties of tetragonal phase Pb $(Mg_{1/3}Nb_{2/3})O_3$–$PbTiO_3$ (PMN–PT) solid solutions have been investigated. The coercivity, E_c, increases monotonically with PT content. The remanent polarization, P_r, on the other hand, decreases rapidly with PT content and reaches a minimum value for a sample containing 0.365 mol% PT. It increases moderately when the PT content is further increased. The deformation parameter, δ, is used to correlate the composition to ferroelectric characteristics of these materials. A critical deformation parameter, $\delta_c = 0.008\,984$, is observed at which the remanent polarization contributed from Mg^{2+} and Nb^{5+} cations, P_r^{MN}, decreases with δ value when $\delta < \delta_c$ and vanishes when $\delta > \delta_c$. The remanent polarization contributed from Ti^{4+} cations, P_r^{Ti}, on the other hand, increases with δ value, following the trend $P_r^{Ti} = k\delta^{1/2}$. The rattling of Mg^{2+} and Nb^{5+} cations among off-centred sites in oxygen octahedra is adapted to explain such a phenomenon.

1. Introduction

Ferroelectricity of simple perovskite materials, such as tetragonal $PbTiO_3$ (PT) and $BaTiO_3$ (BT), are known to originate from the switching of Ti^{4+} cations between two stable off-centred sites of TiO_6^- octahedra in response to an external electric field [1]. The important ferroelectric parameters, such as remnant polarization, P_r, and coercivity, E_c, are intimately related to deformation of the lattice [2]. These materials exhibit marvellous ferroelectric properties only when they are of a non-centrosymmetric structure, such as tetragonal, rhombohedral or orthorhombic. They become paraelectric when the crystal structure transforms from tetragonal to cubic.

The $A(B'B'')O_3$ type perovskites, such as $Pb(Mg_{1/3}Nb_{2/3})O_3$(PMN), on the other hand, still possess remarkable ferroelectric properties even when the materials are of pseudo-cubic structure [3]. Several mechanisms have been proposed [4–9] to account for such an unusual phenomenon. The most plausible one is the rattling of Mg^{2+} and Nb^{5+} cations, namely the cations are distributed in the octahedral sites of perovskite and displaced off-centrally to one of the six [0 0 1] directions in a random manner such that the crystals possess cubic structure even though they can respond to the applied electric field and exhibit large polarization. The same mechanism makes these materials exhibit distinctly different phase-transformation characteristics, from that of simple perovskite materials, which shows diffused phase transition (DPT) characteristics. The materials are rendered paraelectric for a temperature higher than the DPT temperature, where the Mg^{2+} and Nb^{5+} cations are at the centre of the octahedra.

The diffused phase transition (DPT) temperature can be shifted by adding $PbTiO_3$ to $Pb(Mg_{1/3}Nb_{2/3})O_3$ and a solid solution forms [10]. Most of the efforts are, however, focused on the modification of dielectric properties due to PT incorporation and the room-temperature dielectric constant of the materials has been increased markedly, but the response of the individual cations to the external electric field has not been thoroughly investigated. It is therefore of interest to examine the ferroelectric behaviour of cations, especially the Mg^{2+} and Nb^{5+} ions whenever the crystal structure of the PMN–PT solid solution changes from pseudo-cubic to tetragonal with increasing c/a value.

2. Experimental procedure

The $(1 - x)$PMN–xPT solid solutions of the composition $x = 0.29$–0.47, where PMN and PT are $Pb(Mg_{1/3}Nb_{2/3})O_3$ and $PbTiO_3$ perovskite, respectively, were used in this study. They are labelled a_0–a_9 and are listed in Table I. Because the preparation of PMN materials via the mixed oxide route is difficult due to the inevitable formation of stable pyrochlore phase [11–13], spray pyrolysis of the solution technique was adapted in this study to prepare the PMN–PT materials. Atomic-scale mixing in solution is expected to be able to improve the homogeneity of the materials, and the formation of pyrochlore ($Pb_3Nb_4O_{13}$, $Pb_3Nb_2O_8$) compound can hopefully be suppressed. The molar fraction of $PbTiO_3$ was chosen such that the tetragonality of PMN–PT solid solution increases gradually from cubic to tetragonal structure, because the morphotropic phase boundary (MPB) has been reported to be in the region $x = 0.3$–0.325.

In the spray pyrolysis of alkoxide solution process, the niobium ethoxide was first prepared, following the

0022–2461 © *1993 Chapman & Hall*

TABLE I Crystal structure, lattice constant, T_c, P_r and E_c of 1250° C sintered samples

Sample	x^{PT}	Crystal structure	c (nm)	a (nm)	$(a^2c)^{1/3}$ (nm)	T_c (° C)	P_r (μC cm^{-2})	E_c (kV cm^{-1})
a_0	0.29	Cubic	0.4028	0.4028	0.4028	138	25.49	4.18
a_1	0.32	Tetragonal	0.4032	0.4016	0.4021	158	25.49	4.45
a_2	0.335	Tetragonal	0.4034	0.4002	0.4013	166	25.07	4.90
a_3	0.35	Tetragonal	0.4048	0.4000	0.4016	174	22.26	5.70
a_4	0.365	Tetragonal	0.4052	0.3998	0.4016	202	16.15	6.71
a_5	0.38	Tetragonal	0.4056	0.3998	0.4017	206	16.74	8.18
a_6	0.395	Tetragonal	0.4054	0.3989	0.4011	210	18.40	8.96
a_7	0.42	Tetragonal	0.4054	0.3984	0.4007	214	17.14	9.73
a_8	0.44	Tetragonal	0.4048	0.3976	0.4000	226	17.48	12.92
a_9	0.47	Tetragonal	0.4056	0.3978	0.4004	238	17.78	14.75

TABLE II Calculated deformation parameter and polarization of the components of 1250 °C sintered samples

Composition	Deformation parameter, δ	Total polarization, (μC cm^{-2})	X^{PT}	X^{PMN}	P_r^{Ti} ($= k\delta^{1/2}$) (μC cm^{-2})	P_r^{MN} (μC cm^{-2})
a_0	0	25.49	0.29	0.71	0	35.90
a_1	0.002 654	25.49	0.32	0.68	18.69	28.69
a_2	0.005 323	25.07	0.335	0.665	26.47	24.37
a_3	0.007 984	22.26	0.35	0.65	32.41	16.80
a_4	0.008 984	16.15	0.365	0.635	34.38	5.66
a_5	0.009 648	16.74	0.38	0.62	35.63	5.16
a_6	0.010 833	18.40	0.395	0.605	37.75	3.49
a_7	0.011 678	17.14	0.42	0.58	39.20	1.17
a_8	0.012 036	17.48	0.44	0.56	39.80	0
a_9	0.013 029	17.78	0.47	0.53	40.40	0

reaction

$$NbCl_5 + 5C_2H_5OH + 5(C_2H_5)_3N \rightarrow Nb(OC_2H_5)_5 + 5(C_2H_5)_3NCHCl\downarrow \quad (1)$$

The obtained solution was then filtered and stabilized with ethylene glycol and citric acid to prevent the hydrolysis of niobium ethoxide [14]. The titanium butaoxide, lead acetate, and magnesium acetate in the correct amounts were then added to niobium ethoxide. All the chemicals were of reagent grade (Merck Co., Darmstadt, Germany). The mixtures were then sprayed into a hot zone (850 °C) using nitrogen as carrier gas. The pyrolysed powders, which were black in colour, containing a large amount of charred hydrocarbons, were then fired at 900 °C to convert the mixture into oxide powders. The powders obtained were then pressed into pellets and sintered at 1000–1250 °C for 2 h.

The phase and microstructure of the sintered samples were examined by X-ray diffractometry (XRD) and scanning electron microscopy (SEM), respectively. The temperature dependence of dielectric property, K–T, was measured using an H.P. 4194 impedance analyser and the ferroelectric hysteresis loop (P–E curve) was measured using the Sawyer–Tower technique.

3. Results

The X-ray diffraction patterns of $(1 - x)$PMN–xPT materials ($x = 0.29$–0.47), represented by a_0, a_1, a_5, and a_9 samples, are shown in Fig. 1. The Sample a_0 is of cubic structure, and the others are of tetragonal structure. The MPB at room temperature occurs at composition $x = 0.29$–0.32. This is in agreement with the results of, Choi *et al.* [15], Shrout *et al.* [16] and Ouchi *et al.* [10]. The variation of (0 0 2) and (2 0 0) diffraction peaks with temperature of Samples a_0, a_1, a_2, and a_3, shown in the insert of Fig. 1, reveals that the tetragonal to pseudo-cubic transition temperature increases with PT content and the morphotropic phase boundary (MPB) shifts to the larger PT side at higher measuring temperature. The lattice parameters, c, a and cell volume $(a^2c)^{1/3}$ are calculated from the XRD patterns and are plotted in Fig. 2a. In the same figure, a new parameter related to the lattice constant of the tetragonal crystal, defined according to

$$\delta = \frac{c - (a^2c)^{1/3}}{(a^2c)^{1/3}} \quad (2)$$

is also plotted against the PT content. This was called the deformation parameter by Fesenko *et al.* [2] and its significance will be discussed later.

The microstructure of 1250 °C sintered samples, represented, again, by that of Samples a_0, a_1, a_5, and a_9, is shown in Fig. 3. The size of the grain is small (~4 μm) for cubic materials (Sample a_0). It is uniformly large (~10 μm) and the size increases with PT content for tetragonal materials, represented by the microstructure of Samples a_5 and a_9 (Fig. 3c and d). Interestingly, the materials of the composition near MPB (a_1) possess bimodal microstructure, i.e. some

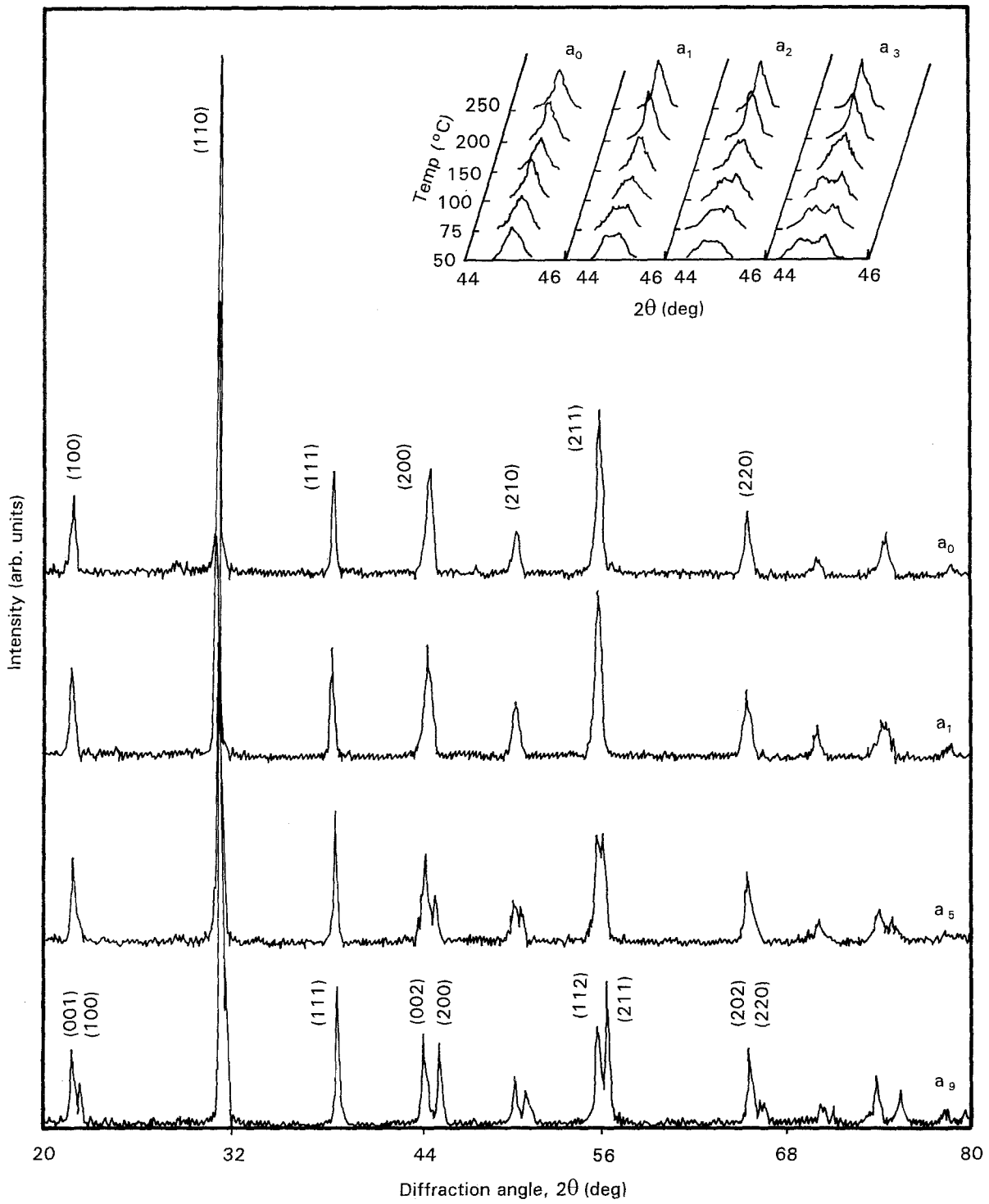

Figure 1 X-ray diffraction patterns of $(1-x)$PMN–xPT materials sintered at 1250 °C for 2 h, with $x = 0.29$ (a_0), 0.32 (a_1), 0.38 (a_5) and 0.47 (a_9), respectively.

small grains (~4 μm) coexists with large grains (~9 μm), as shown in Fig. 3b. It is possibly caused by the coexistence of the two phases in these materials, but is difficult to analyse directly because the detectability of XRD technique of minor phases is limited. The same phenomenon is also observed when the samples are sintered at 1200 °C. The variation of grain size with sintering temperature is plotted in Fig. 2b.

The temperature dependence of dielectric properties of these materials, represented by that of Samples a_0, a_1, a_5, and a_9 only, are plotted in Fig. 4. The DPT characteristics are clearly observed for cubic materials (a_0) and the Curie peaks are sharper for tetragonal materials (a_1–a_9). For ferroelectrics with diffuse phase transition, the Curie–Weiss law $1/K \approx (T - T_c)/C$ is modified. A parameter, Δ, in the expression

$$1/K \approx 1/K_{max} + (T - T_c)^2/2K_{max}\Delta^2 \quad (3)$$

can be used to evaluate the diffuseness of the materials response, assuming that the local Curie temperature distribution is Gaussian in nature [4], where T is temperature, T_c is the Curie point, and K_{max} is the maximum dielectric constant. The results are shown as a dotted line in Fig. 2c. The diffuseness, Δ, drops abruptly when composition changes from a_0 to a_1 and

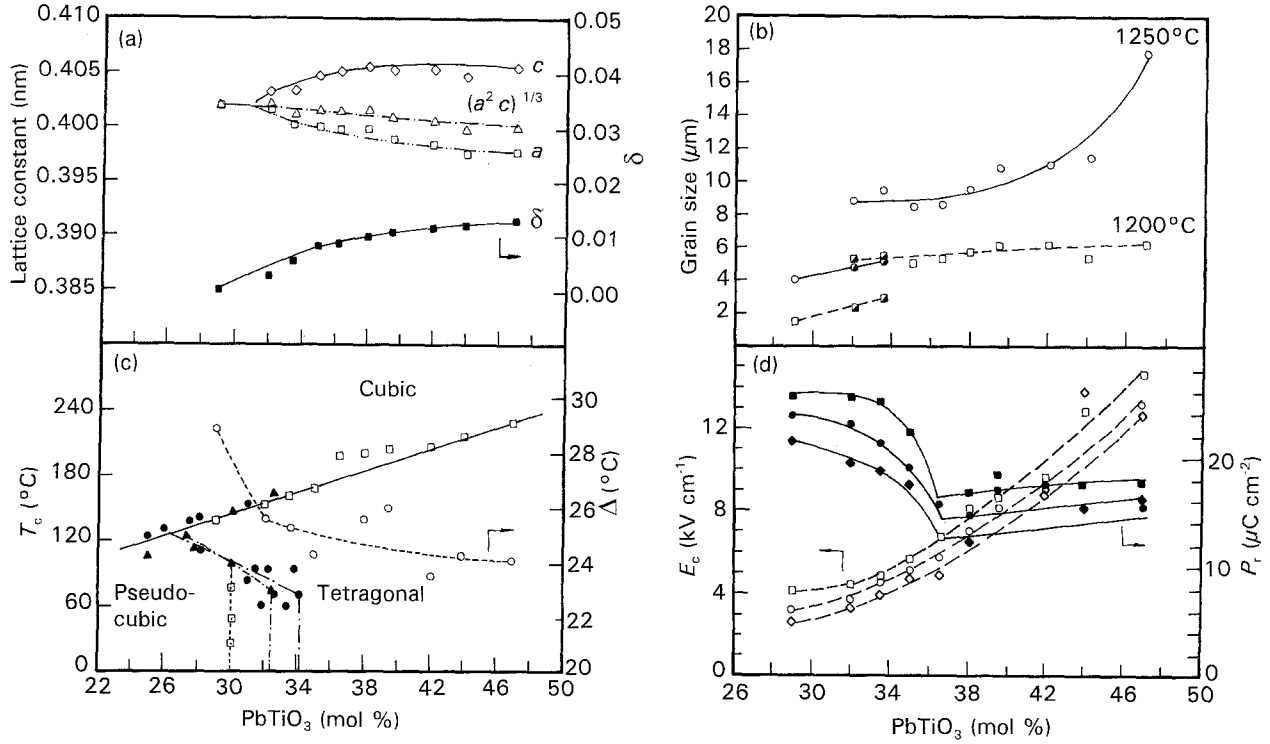

Figure 2 The compositional dependence (PT mol %) of (a) lattice parameters, a, c, and deformation parameters, δ, (b) grain size, (c) diffuseness, Δ, and Curie temperature, and (d) remanent polarization, P_r, and coercivity, E_c. The half (b) (◕, ◪) Both coarse and fine grains coexist. (c) (▲, ●) Data reported by Choi [15] and Shrout [16], respectively, (□, ⊡) present work. (d) Testing temperature: (■, □) 25 °C, (●, ○) 65 °C, (◆, ◇) 100 °C.

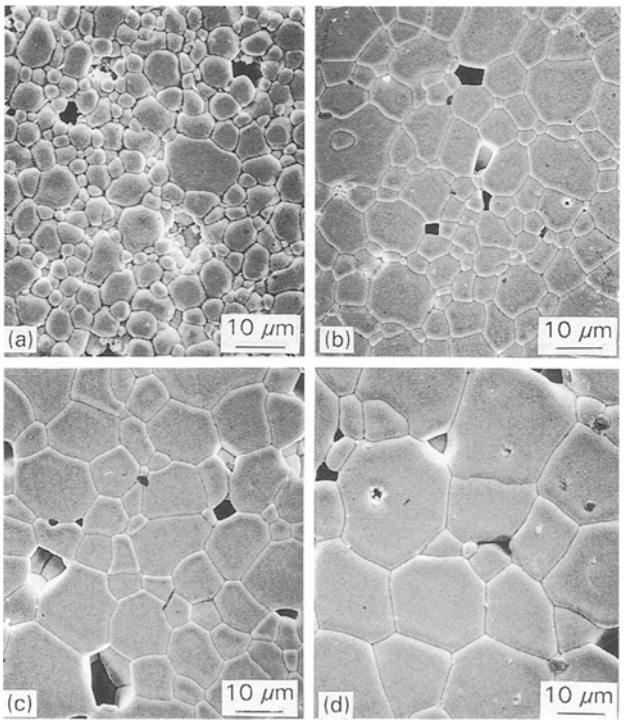

Figure 3 Microstructure of (1 − x)PMN–xPT materials for (a) a_0, (b) a_1, (c) a_5, (d) a_9, sintered at 1250 °C.

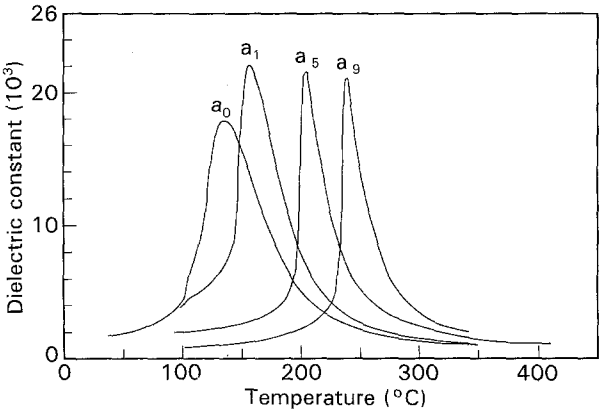

Figure 4 Temperature dependence of dielectric constant of (1 − x) PMN–xPT materials, measured at 1 kHz.

it varies insignificantly thereafter. When the PT proportion increases from a_1 to a_9, the Curie temperature, on the other hand, increases slowly with concentration of PT, as also shown in Fig. 2c.

All of the samples possess good ferroelectric properties. The hysteresis loop is slim and of high squareness for the cubic sample (a_0). It is more slanting and of less squareness for samples containing higher PT (a_1–a_9). Typical P–E curves, represented by that of Samples a_0, a_1, a_5 and a_9, are shown in Fig. 5a. The remanent polarization, P_r, and coercivity, E_c, of the samples, measured at 25, 65 and 100° C, respectively, are plotted in Fig. 2d, which reveals that there are two regions in the composition where the ferroelectric properties vary with content of $PbTiO_3$ in a significantly different manner. In the low-PT region, the remanent polarization, P_r, decreases rapidly and reaches a minimum value, while in the high-PT region, the P_r value increases only slightly with PT content. The coercivity, E_c, on the other hand, increases monotonically with concentration of PT.

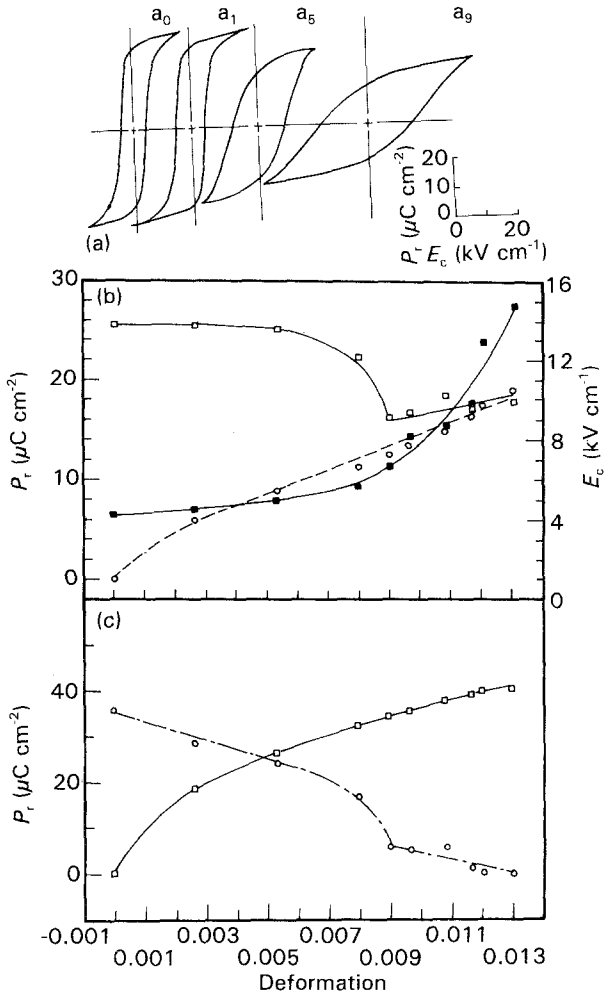

Figure 5 (a) Ferroelectric hysteresis loop of a_0, a_1, a_5, a_9 PMN–PT materials and the variation of (b) (□) total polarization P_r^T, (■) coercivity E_c and (○) $P_r^{Ti}x^{Ti}$, and (c) (□) Ti^{4+} ion contribution, P_r^{Ti}, and (○) magnesium-niobium Mg^{2+}, Nb^{5+}-ion contribution, P_r^{MN}, to the total polarization, with deformation parameters, δ.

4. Discussion

A similar compositional dependence of dielectric and pyroelectric properties of PMN–PT solid solution to that shown in Fig. 2d has also been obtained by Choi *et al.* [15] and Shrout *et al.* [16]. They observed that the spontaneous polarization, P_s, exhibits a maximum value at the pseudo-cubic and tetragonal phase boundary, decreases rapidly when the composition deviates from MPB with a minimum value occurring at 0.35 mol % PT composition, and the P_s value changes moderately in a reverse manner thereafter. While the increase of coercivity with PT content can be ascribed to the monotonic increase in c/a ratio, the variation of P_s value with composition in the materials is not as evident.

To examine the influence of PT content on the polarization of the samples, the characteristic parameters (P_r and E_c), derived from the hysteresis loop of the samples in Fig. 5a, are replotted against the deformation parameters and are shown in Fig. 5b. The remanent polarization, P_r, instead of saturated polarization, P_s, is used for further discussion, because it is the polarization related to the deformation parameters measured at zero applied electric field. It is clearly indicated that there are two distinct regions in P_r–δ and E_c–δ plots. The P_r value decreases quickly with increasing PT content for low deformation region (I), and it increases moderately with PT content for the high deformation region (II). The coercivity increases monotonically with PT content but the slope changes when the composition of the samples shifts from one region to the other.

The polarization value contributed by the PT and PMN phases will then be estimated, assuming that the polarizations of the two phases are additive, i.e.

$$P^{total} = P_r^{Ti}x^{PT} + P_r^{MN}x^{PMN} \quad (4)$$

where P_r^{Ti}, P_r^{MN} are polarization values of PT and PMN phases, respectively. The spontaneous polarization of tetragonal perovskites, such as $PbTiO_3$ and $BaTiO_3$, have been proposed by Fesenko *et al.* [2] to be related to the deformation parameters, defined in Equation 2 by the formula

$$P_s^{Ti} = k\delta^{1/2} \quad (5)$$

where $k = (1 \times 10^7)^{1/2}$. The same relationship is expected when the $PbTiO_3$ is partially replaced by PMN and will be used to calculate the contribution of PT to the total polarization of the PMN–PT solid solution.

The P_r value contributed from the PT phase is calculated using the formula $P_2 = P_r^{Ti}x^{PT}$, where x^{PT} is the mole fraction of the phase. The results are shown in Fig. 5b and it clearly shows that the polarization of the solid solution in the high deformation region (II) is very close to that of the PT phase in this region. The polarization value of PMN phase, P_r^{MN}, can then be estimated from Equation 4 and the results are shown in Fig. 5c. The deformation parameter, δ, dependence of P_r^{MN} is quite different from that of P_r^{Ti}, i.e. polarization of tetragonal perovskite ($PbTiO_3$). The polarization of PMN phase, P_r^{MN}, decreases as the deformation parameter, δ, increases, while that of the PT phase, P_r^{Ti}, increases with δ according to Equation 5. To understand the mechanism which results in decreasing δ-parameter dependence of the P_r value, the source of polarization of PMN materials should be re-examined. In $PbTiO_3$ materials, the TiO_6^- octahedra exhibit marked polarization only when the deformation parameter is non-zero ($\delta \neq 0$) and the Ti^{4+} ions in the octahedron are off-centred. In other words, these materials are ferroelectric in the tetragonal phase and are paraelectric in the cubic phase. On the contrary, the pseudo-cubic PMN materials show remarkable ferroelectricity and high remanent polarization at low temperature ($T < -10\,°C$), even though the crystals are of cubic symmetry and of zero δ value.

This peculiar behaviour of PMN materials, is expected to come from the same origin as that resulting in the unique diffused phase transition (DPT) characteristics of the materials. Among the mechanisms which have been proposed [4–9] for explaining the DPT behaviour of PMN materials, the rattling of cations [5] inside the octahedra formed by oxygen anions seems to be the most plausible to account for the above-mentioned phenomenon. In other words, the Mg^{2+} and Nb^{5+} cations in their octahedra are assumed, microscopically, off-centred, but the cations

are displaced towards one of the six oxygen ions in a random manner such that even though each octahedron is slightly distorted, the unit cell of the crystal is still of cubic symmetry at zero applied electric field. They can still, however, respond to applied field and jump among nearby off-centred sites in the same octahedron in order to induce large polarization and electrostriction. A marvellous ferroelectric hysteresis thus results even though the crystals are of cubic symmetry.

The decrease of P_r with δ, on the other hand, is possibly due to the difficulty of the cations to jump between off-centred sites in the deformed lattice. The ionic size of Mg^{2+} and Nb^{5+} ions is so large ($r_{Mg2+} = 0.072$ nm and $r_{Nb5+} = 0.064$ nm) that the switching in off-centred sites is impeded significantly whenever the unit cell is deformed. The larger the deformation parameter, δ, in the tetragonal phase, the more difficult it is for these cations to jump. It is expected that those large Mg^{2+} and Nb^{5+} ions will be frozen at one of the [0, 0, $\pm \varepsilon$] off-centre sites of the octahedron completely whenever the δ parameter is larger than a critical value, which is estimated as $\delta_c = 0.008\,984$ for PMN–PT solid solution. Beyond this value, only the smaller Ti^{4+} ions ($r_{Ti4+} = 0.0605$ nm) can still jump around cooperatively and contribute to the polarization of the PMN–PT solid solution such that the polarization value moderately increases with PT content for samples with δ greater than the critical value.

On the contrary, the coercivity, E_c, of the PMN–PT solid solution increases monotonically with δ, with a change in slope at δ_c. Because the coercive force represents the energy barrier which the small cations must overcome to jump from one of the off-centred sites to the other in the same octahedron, the cations which encounter the highest jump barrier will need the largest external field to switch the occupying sites and determine the E_c-value of the sample. When δ is below the critical value, all of the three cations are active, the δ-dependence of coercivity is possibly predominated by that of the largest cation, Mg^{2+} (0.072 nm). When $\delta > \delta_c$, the Mg^{2+} and Nb^{5+} cease to respond to the electric field, the δ-dependence of Ti^{4+} ions will take over the electrical response of the materials.

Above all, the P_r–δ and E_c–δ relationships infer that in PMN–PT solid solution, both of the Mg^{2+}/Nb^{5+} cations and Ti^{4+} cations contribute to the ferroelectric properties of the materials. In the low deformation region ($\delta < \delta_c$), the Mg^{2+}/Nb^{5+} cations predominate the remanence, P_r, and coercivity, E_c, of the sample, while in the high deformation region ($\delta > \delta_c$), the Mg^{2+}/Nb^{5+} cations cease to respond to the external field such that the Ti^{4+} cations determine the ferroelectricity of the sample.

5. Conclusions

Ferroelectric properties of $(1 - x)$PMN–xPT solid solution have been examined and the morphotropic phase boundary (MPB), as determined from X-ray diffraction patterns, microstructure and dielectric properties, is located at $x = 0.29$–0.32.

1. The pseudo-cubic structure materials ($x = 0.29$) possess fine-grained microstructure (~ 4 μm), larger diffuseness ($\Delta \approx 28.8\,^{\circ}C$) and slim ferroelectric loop characteristics. On the other hand, the tetragonal structure materials possess coarse-grained microstructure (~ 10 μm), smaller diffuseness ($\Delta \approx 23.3$–$26\,^{\circ}C$) and more slanting ferroelectric hysteresis curve characteristics.

2. The deformation parameter, δ, is found to be more appropriate to describe the compositional dependence of ferroelectric properties. The remanent polarization, P_r, decreases in the low δ region (I) and increases only slightly in the high δ region, with concentration of PT. The coercivity, E_c, increases monotonically with PT content with a change in slope in the two regions.

3. The polarization contributed by Mg^{2+} and Nb^{5+} cations can be separated from that of Ti^{4+} cations and is observed to decrease as deformation parameter, δ, increases. P_r^{MN} vanishes for the samples with the values of δ beyond the critical value ($\delta_c = 0.008\,984$). The total polarization is then contributed from that of Ti^{4+}-ions only for the $\delta > \delta_c$ region.

4. The coercivity, E_c, of the materials is determined by the switchability of large cations, Mg^{2+}, in the low δ region and is determined by that of small Ti^{4+} cations for the $\delta > \delta_c$ region.

Acknowledgement

The financial support of NSC-80-0404-E-007-10 is greatly appreciated.

References

1. B. JAFFE, W. R. COOK and H. JAFFE, in "Piezoelectric Ceramics" (Academic, New York, 1971) p. 56.
2. E. G. FESENKO, V. S. FILIP'EV and M. F. KUPRIYANOV, *Sov. Phys. Solid State* **11** (1969) 366.
3. V. A. BOKOV and I. E. MYL'NIKOVA, *ibid.* **3** (1961) 613.
4. H. T. MARTIRENA and J. C. BURFOOT, *J. Phys. C Solid State Phys.* **7** (1974) 3182.
5. A. AMIN, R. E. NEWNHAM, L. E. CROSS, S. NOMURA and D. E. COX, *J. Solid State Chem.* **35** (1980) 267.
6. L. E. CROSS, S. J. JANG, R. E. NEWNHAM, S. NOMURA and K. UCHINO, *Ferroelectrics* **23** (1980) 187.
7. G. A. SMOLENSKII, *ibid.* **53** (1984) 129.
8. B. N. ROLOV, *Sov. Phys. Solid State* **6** (1965) 1676.
9. L. E. CROSS, *Ferroelectrics* **76** (1987) 241.
10. H. OUCHI, K. NAGANO and S. HAYAKAWA, *J. Am. Ceram. Soc.* **48** (1965) 630.
11. S. L. SWARTZ and T. R. SHROUT, *Mater. Res. Bull.* **17** (1982) 1245.
12. J. P. GUHA and H. V. ANDERSON, *J. Am. Ceram. Soc.* **69** (1986) c-287.
13. H. S. HOROWITZ, *ibid.* **71** (1980) c-250.
14. M. PECHINI, US Pat. 3330 697, 11 July, 1967.
15. S. W. CHOI, T. R. SHROUT, S. J. JANG and A. S. BHALLA, *Ferroelectrics* **100** (1989) 29.
16. T. R. SHROUT, Z. P. CHANG and S. MARKGRAF, *Ferroelect. Lett.* **12** (1990) 63.

Received 4 June 1992
and accepted 3 February 1993